

Revisiting the Stokes-Einstein relation without a hydrodynamic diameter

Cite as: J. Chem. Phys. 150, 021101 (2019); doi: 10.1063/1.5080662

Submitted: 10 November 2018 • Accepted: 17 December 2018 •

Published Online: 10 January 2019



View Online



Export Citation



CrossMark

Lorenzo Costigliola,^{1,a)} David M. Heyes,² Thomas B. Schröder,¹ and Jeppe C. Dyre^{1,b)}

AFFILIATIONS

¹“Glass and Time,” IMFUFA, Department of Science and Environment, Roskilde University, P.O. Box 260, DK-4000 Roskilde, Denmark

²Department of Mechanical Engineering, Imperial College London, Exhibition Road, South Kensington, London SW7 2AZ, United Kingdom

^{a)}lorenzo.costigliola@gmail.com

^{b)}dyre@ruc.dk

ABSTRACT

We present diffusion coefficient and shear viscosity data for the Lennard–Jones fluid along nine isochores above the critical density, each involving a temperature variation of roughly two orders of magnitude. The data are analyzed with respect to the Stokes–Einstein (SE) relation, which breaks down gradually at high temperatures. This is rationalized in terms of the fact that the reduced diffusion coefficient \tilde{D} and the reduced viscosity $\tilde{\eta}$ are both constant along the system's lines of constant excess entropy (the isomorphs). As a consequence, $\tilde{D}\tilde{\eta}$ is a function of $T/T_{\text{Ref}}(\rho)$ in which T is the temperature, ρ is the density, and $T_{\text{Ref}}(\rho)$ is the temperature as a function of the density along a reference isomorph. This allows one to successfully predict the viscosity from the diffusion coefficient in the studied region of the thermodynamic phase diagram.

Published under license by AIP Publishing. <https://doi.org/10.1063/1.5080662>

In a computer simulation, the self-diffusion coefficient is easily found from the long-time mean-square displacement, whereas determining the (shear) viscosity is much more involved.^{1,2} Relating these two quantities is consequently of great practical importance. It is also interesting from a theoretical perspective, and the relation between the self-diffusion of particles in a liquid and the viscosity has been the subject of intense investigation over many decades. The Einstein–Smoluchowski–Sutherland relation states³ that

$$D = \mu k_B T. \quad (1)$$

Here D is the particle's diffusion coefficient, μ is its mobility, i.e., the average velocity over force in the linear limit, k_B is the Boltzmann constant, and T is the temperature. In modern language, Eq. (1) simply expresses the fluctuation-dissipation theorem.

A macroscopic particle in a liquid subject to a small external force is associated with a low Reynolds number (non-turbulent) flow. The mobility of the particle is consequently

described by Stokes' law,³ and the mobility is related to the size of the particle through its hydrodynamic diameter σ_H by (in which c is a numerical constant)

$$\mu = \frac{1}{c\pi\eta\sigma_H}. \quad (2)$$

Combining Eqs. (1) and (2) gives a relation between D and η , the famous Stokes–Einstein (SE) relation valid for the diffusion coefficient of large spherical particles,^{4,5}

$$D\eta = \frac{k_B T}{c\pi\sigma_H}. \quad (3)$$

The dimensionless quantity c is given^{6,7} by

$$c = 3 \frac{1 + 4\eta/\beta\sigma_H}{1 + 6\eta/\beta\sigma_H}, \quad (4)$$

in which β is the so-called coefficient of sliding friction. The “slip” boundary condition case corresponds to $\beta \rightarrow 0$, giving $c = 2$, while $c = 3$ is the “stick” boundary condition of high sliding friction ($\beta \rightarrow \infty$).

The above considerations apply for a macroscopic particle in a continuum. Numerous molecular dynamics (MD) simulations and experiments have shown, however, that the SE relation applies reasonably well even for tracer molecules of similar size to the solvent molecules although the SE relation is not exact and deviations from it are consistently found (below, the particles are referred to as molecules when tracer and solvent are distinguished).⁸⁻¹² These deviations have been variously interpreted as being due to the fact that

- the parameter c for different thermodynamic conditions may change between its slip and stick limits;⁶
- the local “microviscosity” experienced by a tracer molecule is not the same as the viscosity of the bulk liquid;¹³⁻¹⁵
- the effective hydrodynamic diameter depends in a non-trivial way on the chemistry, the physical diameters of the tracer and solvent molecules, and the fluid density.^{8,16}

Since a combination of all three explanations could be present in any given case, it is difficult to make progress in resolving the cause(s) of departure from the SE relation.

MD simulations show¹⁷ that as the mass ratio (MR) and diameter ratio (DR) of the tracer to solvent molecule increase, the diffusion coefficient eventually reaches the hydrodynamic limit and becomes essentially independent of these quantities. There is a strong coupling between the two ratios, however. For example, MD simulations indicate that this limit is reached when DR = 4 for MR = 5, and when DR = 0.5 the limit is achieved by MR = 40. The c variable tends toward the slip limit when the tracer molecule is smooth and interacts mainly repulsively with the solvent molecules,¹⁸ but c tends toward the stick limit when the tracer is rough and/or has a strong attraction for the solvent molecules.¹⁹⁻²¹ With increasing host fluid density, c typically increases.^{16,19,22-24}

There is often a pronounced breakdown of the SE relation in supercooled liquids.²⁵⁻²⁷ The applicability of the SE relation for tracer molecules similar to those of the solvent has prompted attempts to rationalize this breakdown in terms of liquid-state statistical mechanics.²⁸⁻³⁰ Another approach to accommodate departures from the SE relation for small tracer molecules has been to assume that $(D/T) \eta^p = \text{constant}$,³¹ in which $p < 1$. This so-called fractional SE relation applies to molecular fluids and ionic liquids, and interestingly one finds that p is usually independent of both pressure and temperature.^{32,33} The fractional SE relation was applied to supercooled liquids in Refs. 31 and 33-35.

It has been found that the SE relation is more likely to apply for a liquid close to the melting temperature than at higher temperatures; see, for example, the MD results for model rubidium in Ref. 36 and the analysis of experimental data in Refs. 37 and 38. This is confirmed by the simulations reported below. Zwanzig³⁹ derived a variant of the SE relation based on a number of assumptions about the molecular dynamics of the tracer diffusion mechanism, arriving at a formula that had been previously proposed

by more semi-empirical routes.^{7,40,41} In this modification of the SE relation, the effective hydrodynamic diameter σ_H is replaced by $\rho^{-1/3}$ in which, for N molecules in volume V , $\rho = N/V$ is the number density. Equation (3) is then transformed into the following dimensionless version:

$$\frac{D\eta}{\rho^{1/3} k_B T} = \frac{1}{c\pi} \equiv \alpha. \quad (5)$$

The hydrodynamic theory for macroscopic spheres in Eq. (3) gives α ranging from 0.106 for stick to 0.159 for slip boundary conditions. A subsequent analysis of Eq. (5) was given in Ref. 42. More recently, Ohtori and Ishii suggested that the $\rho^{1/3}$ term arises from the presence of voids in the liquid that are not incorporated in the continuum description used for macroscopic “tracer” spheres.^{43,44} Very recently, the same authors have studied the SE relation for the Lennard-Jones (LJ) liquid in coexistence with the gas phase and confirmed this form of scaling in a paper that also provides a useful brief review of the history of the SE relation.⁴⁵

Jakse and Pasturel⁴⁶ considered the validity of the SE relation in the context of model liquid alloys studied by MD simulations involving little density variation. Their data were analyzed using Rosenfeld’s excess-entropy scaling theory,⁴⁷ in which the reduced transport coefficients are exponential functions of the excess entropy. They concluded that the quantity $D\eta/k_B T$ depends only on the excess entropy. Moreover, they found that the hydrodynamic diameter obtained from the SE relation does not agree well with the actual size of the alloy components. Binary mixtures were also simulated by Puosi *et al.*²⁷ who showed that the Debye-Waller factor, which quantifies the short-time plateau in the mean-square displacements, in glassy systems correlates with the product $D\eta$. The results of these two recent studies are consistent with the arguments developed below.

This paper presents extensive numerical data investigating the SE relation and its breakdown for the Lennard-Jones (LJ) system {the LJ pair potential is given by $v(r) = 4\epsilon[(r/\sigma)^{-12} - (r/\sigma)^{-6}]$ ⁴⁸}. We show that the parameter α in Eq. (5) is constant along the configurational adiabats, the lines of constant excess entropy in the thermodynamic phase diagram. These lines are termed “isomorphs” when the system has the property that the microscopic dynamics is invariant along the configurational adiabats.⁴⁹

Figure 1(a) shows the state points simulated in the standard LJ unit system defined by the pair-potential parameters ϵ and σ (both set to unity in the simulations). Nine isochores were studied. At all state points, $N = 1000$ particles were simulated. The simulations were carried out using the graphical processing unit (GPU) code RUMD (Roskilde University Molecular Dynamics)⁵² with a shifted-potential cutoff at 2.5σ . The time step was adjusted such that the reduced time step (see below) was 0.001 in all simulations.⁵³ At each state point, the system was simulated for at least $5 \cdot 10^8$ time steps.

Two simulations were performed at each state point: an NVT simulation determined the mean-square displacement from which the diffusion coefficient was extracted, while a

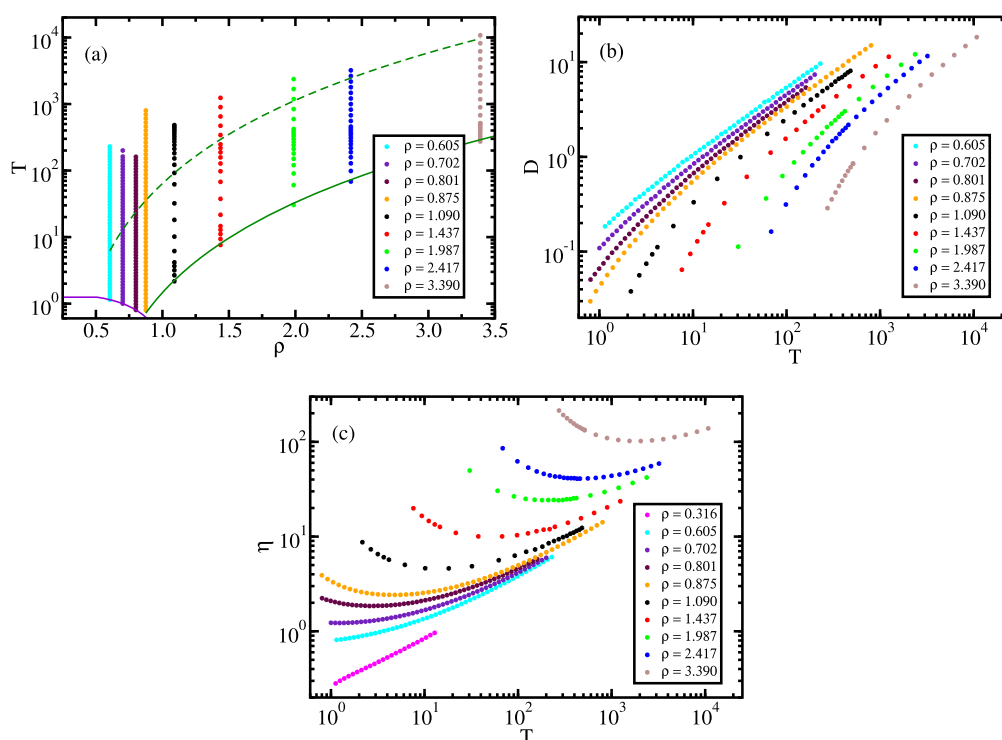


FIG. 1. Simulations of the Lennard-Jones fluid over a broad range of densities and temperatures above the critical density. The diffusion coefficient and viscosity were calculated for state points on nine isochores. The numerical data are available from the data repository at <http://glass.ruc.dk>. (a) shows the state points studied. The lowest temperature on each isochore is either on the gas-liquid coexistence line (low densities, purple curve)⁵⁰ or on the freezing line (high densities, full green line).⁵¹ On each isochore, the highest temperature simulated is about two orders of magnitude larger than the lowest temperature. The green dotted line marks the reference isomorph detailed below; the reference-isomorph temperature as a function of the density is in the following denoted by $T_{\text{Ref}}(\rho)$. (b) Diffusion coefficient D as a function of temperature along the nine isochores. At each state point, D was evaluated from the long-time limit of the mean-square displacement in an NVT simulation. (c) Viscosity η along the nine isochores calculated from SLLOD simulations as described in the text. Data for the critical isochore are also reported in (c). - Lennard-Jones units are used in (a), (b), and (c).

SLLOD simulation^{54–56} determined the viscosity as the low-shear-rate limit of the steady state viscosity. More details on how we obtained the viscosity from SLLOD simulations can be found in the Appendix of Ref. 53. Based on the statistical noise, we estimate the reported viscosities to be accurate within 10%, with the largest errors occurring at the highest temperatures. Figures 1(b) and 1(c) show the temperature dependence of D and η , respectively, along each of the nine isochores. While D increases monotonically with T , η initially decreases and then starts to increase.

Equation (3) has been used broadly in the literature, assuming that the liquid particles can be approximated by hard spheres of constant diameter. Figure 2(a) shows all our numerical data by plotting the diffusion coefficient versus the viscosity. The question addressed now is how to rationalize the two orders of magnitude data variation of this figure. In Fig. 2(b), the quantity $D\eta/(k_B T)$ is plotted as a function of the temperature for all state points. If c and the hydrodynamic diameter σ_H in Eq. (3) were constant, all data would collapse onto a horizontal line, which is evidently not the case. The figure shows that $D\eta/(k_B T)$ is generally larger at high temperatures than at low. On each isochore, this quantity has a shallow minimum

as a function of the temperature. This explains why the SE relation appears to hold in part of the thermodynamic phase diagram.

The isomorph theory⁵⁸ is a consequence of the “hidden scale invariance” condition that the ordering of potential energies of system configurations at one density is maintained if these are scaled uniformly to a different density.⁵⁹ If $U(\mathbf{R})$ is the potential energy with all particle coordinates defining the vector \mathbf{R} , hidden scale invariance is defined by the following logical implication: $U(\mathbf{R}_a) < U(\mathbf{R}_b) \Rightarrow U(\lambda\mathbf{R}_a) < U(\lambda\mathbf{R}_b)$. The term “hidden” refers to the fact that this property is rarely obvious from the expression for $U(\mathbf{R})$. Although the hidden-scale-invariance property is only approximate for realistic systems like the LJ system, its consequences have nevertheless been found to apply to good approximation for many systems.^{49,58–60}

The thermodynamic phase diagram of a Roskilde (R)-simple system (one that has hidden scale invariance to a good approximation⁴⁹) is basically one-dimensional in regard to structure and dynamics. This is because the dynamics in reduced units is invariant along the curves of constant excess entropy, the system’s so-called isomorphs. Most van der Waals

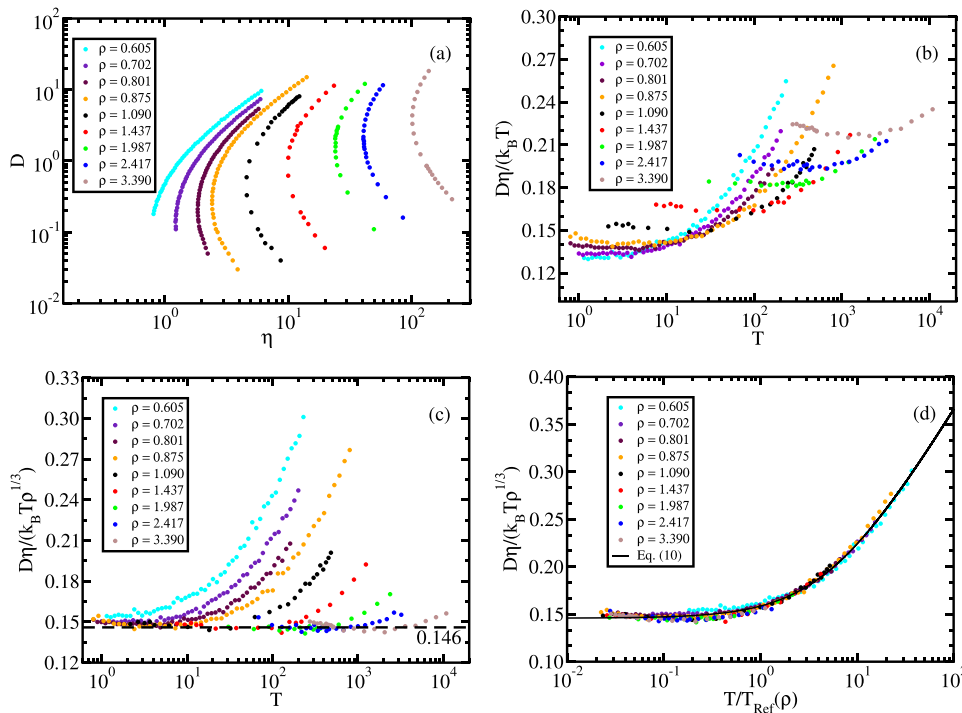


FIG. 2. (a) Diffusion coefficient versus viscosity for all state points studied. (b) Test of the Stokes-Einstein (SE) relation Eq. (3) for the LJ system, according to which a constant hydrodynamic diameter implies a constant $D\eta/(k_B T)$. Clear deviations from this are observed, notably at high temperatures. Nevertheless, the SE relation reduces the variation from the two orders of magnitude in (a) to a factor of two. (c) Plot of $\tilde{D}\tilde{\eta} = D\eta/(k_B T\rho^{1/3})$ as a function of T for all state points [Eq. (8)]. At low temperatures, the data collapse, corresponding to a hydrodynamic diameter that is constant in reduced units, i.e., scales with density as $\rho^{-1/3}$. This “reduced” version of the SE relation breaks down, however, at high temperatures. The constant level at low temperatures is close to the slip-boundary condition prediction (see the text). (d) Plot of $\tilde{D}\tilde{\eta} = D\eta/(k_B T\rho^{1/3})$ as a function of $T/T_{\text{Ref}}(\rho)$, in which $T_{\text{Ref}}(\rho)$ is the temperature’s variation along the reference isomorph (see below). The observed collapse is predicted by the isomorph theory. The full line is the analytical fit given in Eq. (10).

bonded systems and metals are R-simple, whereas systems with strong directional bonds, like hydrogen- or covalently bonded systems, are not. Indeed, the latter systems have long been known to be more complex in regard to structure, dynamics, and thermodynamics, with water as an outstanding example violating many empirical rules that apply for simple liquids.⁶¹ The isomorph-theory framework has been applied to explain results from computer simulations of, e.g., single-component and binary LJ-type systems, simple molecular models, single crystals, the thermodynamics of melting and freezing, nano-confined liquids, non-linear shear flows, zero-temperature plastic flows of glasses, polymer-like flexible molecules, metals studied by *ab initio* density-functional-theory computer simulations, plasmas, physical aging, and recently for justifying a quasiuniversal viscosity equation for supercritical R-simple liquids.^{49,59,60}

Reduced quantities have been made dimensionless by reference to the unit system defined by the length unit $l_0 \equiv \rho^{-1/3}$, the energy unit $e_0 \equiv k_B T$, and the time unit $t_0 \equiv \rho^{-1/3}(m/k_B T)^{1/2}$, where m is the particle mass. Henceforth, a tilde indicates that the quantity in question is given in reduced units. For example, the reduced diffusion coefficient \tilde{D} is obtained by dividing D by l_0^2/t_0 , resulting⁵⁸ in

$$\tilde{D} \equiv \rho^{1/3}(m/k_B T)^{1/2} D. \quad (6)$$

Since the viscosity has dimension mass over (length*time), the reduced viscosity is given⁵⁸ by

$$\tilde{\eta} \equiv \rho^{-2/3}(mk_B T)^{-1/2} \eta. \quad (7)$$

From the isomorph-theory perspective, the relevant quantities describing a system are \tilde{D} and $\tilde{\eta}$, not D and η , because \tilde{D} and $\tilde{\eta}$ are both invariant along any isomorph. The “isomorph filter”⁵⁸ is the following rule: if one side of an equation is isomorph invariant, the other side of the equation must also be isomorph invariant—otherwise the equation cannot hold for an R-simple system. Applying this line of reasoning to the SE relation, we divide Eq. (3) by $\rho^{1/3}k_B T$ to obtain

$$\frac{D\eta}{\rho^{1/3}k_B T} = \tilde{D}\tilde{\eta} = \frac{1}{\rho^{1/3}c\pi\sigma_H}. \quad (8)$$

If c is constant, the right-hand side can only be isomorph invariant if $\sigma_H \propto \rho^{-1/3}$. In this way, the isomorph theory provides a theoretical justification of Eq. (5). In Fig. 2(c), we plot $\tilde{D}\tilde{\eta}$ as a function of the temperature. To a good approximation, $\tilde{D}\tilde{\eta}$ is constant in the part of the phase diagram corresponding to (relatively) low temperatures. The constant [α of Eq. (5)] is 0.146, which is close to the value 0.159 predicted for the slip boundary condition in the hydrodynamic treatment.

Note that isomorph theory does not predict that $\tilde{D}\tilde{\eta}$ is constant; it predicts that this quantity can be constant throughout the phase diagram and, crucially, that the quantity $D\eta/k_B T$ cannot be constant. In other words, the SE relation with a constant hydrodynamic diameter is incompatible with isomorph theory and cannot apply for any R-simple system like the LJ system.

The isomorphs are virtually parallel to the freezing line, which is itself an isomorph to a good approximation.^{53,62} In the simplest version of the theory,⁵⁸ isomorphs are identified from

the condition $T/T_{\text{Ref}}(\rho) = \text{Const.}$,⁵⁷ in which $T_{\text{Ref}}(\rho)$ is the temperature of the state point with density ρ on a selected “reference isomorph.” The choice of reference isomorph is arbitrary; compare the supplementary material of Ref. 57. The one used here is shown as the dashed line in Fig. 1(a). For the LJ system, the temperature variation along an isomorph is given^{63,64} by

$$\frac{T(\rho)}{T_0} = \left(\frac{\gamma_0}{2} - 1\right) \left(\frac{\rho}{\rho_0}\right)^4 - \left(\frac{\gamma_0}{2} - 2\right) \left(\frac{\rho}{\rho_0}\right)^2. \quad (9)$$

Here $\gamma_0 \equiv (\partial \ln T / \partial \ln \rho)_{S_{\text{ex}}}$ is the so-called density-scaling exponent evaluated at the selected state point (ρ_0, T_0) on the isomorph; this quantity can be determined from $\gamma_0 = \langle \Delta U \Delta W \rangle / \langle (\Delta U)^2 \rangle$, in which W is the virial and the angular brackets denote canonical (NVT) averages.⁵⁸ The ρ^4 term in Eq. (9) derives from the repulsive r^{-12} term of the LJ pair potential, while the negative ρ^2 term derives from the attractive r^{-6} term of the potential.^{63,64} The reference isomorph was generated from the state point $(\rho_0, T_0) = (1.09, 92.17)$ at which $\gamma_0 = 4.26$.

Since $\tilde{D}\tilde{\eta}$ is constant along the system’s isomorphs, one has $\tilde{D}\tilde{\eta} = f(S_{\text{ex}})$, in which S_{ex} is the excess entropy. Computing this quantity is tedious, and we instead investigate the predicted isomorph invariance of $\tilde{D}\tilde{\eta}$ by plotting in Fig. 2(d) this quantity as a function of $T/T_{\text{Ref}}(\rho)$ in which $T_{\text{Ref}}(\rho)$ is the temperature variation as a function of the density along the reference isomorph. To a good approximation, the quantity $T/T_{\text{Ref}}(\rho)$ identifies the isomorph through the state point (ρ, T) .⁶³ Instead of using as a reference isomorph the freezing line as in Ref. 57, we have chosen an isomorph located at higher temperatures because this allows one to go below the triple point density on the reference isomorph. The data in Fig. 2(d) collapse nicely though not entirely, reflecting the fact that the isomorph theory is not exact. It should be kept in mind, though, that while D and η vary more than two orders of magnitude, the scatter in Fig. 2(d) is less than 10%. We see that the reduced-unit “isomorphic” version of the SE relation, $\tilde{D}\tilde{\eta} = \text{Const.}$, holds at lower temperatures, whereas significant deviations are seen at higher temperatures. Upon increasing the temperature at constant density, deviations from constant $\tilde{D}\tilde{\eta}$ show up when the temperature exceeds $T_{\text{Ref}}(\rho)$. Thus the reference isomorph marks roughly the upper limit of the part of the phase diagram in which the isomorphic version of the Stokes-Einstein relation $\tilde{D}\tilde{\eta} = \text{Const.}$ holds.

The bottom line of the above is that the role of the hydrodynamic diameter is taken by the length defined by density, $l_0 = \rho^{-1/3}$, a measure of the average interparticle spacing. This justifies the approach of Zwanzig and others.^{39,40,43-45} Note that the hydrodynamic diameter identified by Eq. (3) has often been related to the position of the first peak in the two-particle radial distribution function,^{20,22,23} a position that scales with density as $\rho^{-1/3}$ along any isomorph. The black line in Fig. 2(d) is the following empirical fit:

$$\begin{aligned} \tilde{D}\tilde{\eta} &\equiv D\eta / (k_B T \rho^{1/3}) = A + B \ln \left(1 + C T / T_{\text{Ref}}(\rho) \right) \\ &\equiv F(T / T_{\text{Ref}}(\rho)), \end{aligned} \quad (10)$$

with $A = 0.146$, $B = 0.0735$, and $C = 0.189$.

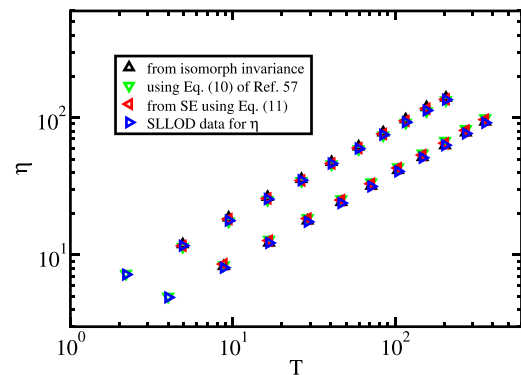


FIG. 3. Comparison between the viscosity along two isomorphs (blue triangles) and the prediction of Eq. (11) (red triangles) based on diffusion coefficient data, determining the isomorph-dependent number $\tilde{D}\tilde{\eta}$ using the analytical fit Eq. (10). The two isomorphs were generated, respectively, from the state point $(\rho, T) = (1.063, 2.2)$ at which $\gamma_0 = 4.89$ (black symbols) and $(\rho, T) = (1.063, 4.0)$ at which $\gamma_0 = 4.76$ (blue symbols). The density of the last point simulated along each isomorph is roughly three times the starting density. The black triangles mark the viscosity predicted from its lowest-density value utilizing the fact that the reduced viscosity is isomorph invariant. The green triangles mark the prediction of the approximate analytical expression for the LJ viscosity of Ref. 57.

Finally, we demonstrate how the fact that the SE breakdown is isomorph invariant may be utilized for predicting viscosities from diffusion coefficients, which are much easier to determine numerically. This is achieved by rewriting Eq. (8) in the following form:

$$\eta = \tilde{D}\tilde{\eta} \frac{\rho^{1/3} k_B T}{D} = F(T/T_{\text{Ref}}) \frac{\rho^{1/3} k_B T}{D}. \quad (11)$$

Equations (10) and (11) allow one to predict how the viscosity varies along an isomorph. As an example, predictions based on Eq. (11) are shown as the red triangles in Fig. 3 along two isomorphs. The predictions compare well to the actual viscosity values (blue triangles). The viscosity is predicted within 6%. For completeness we show also for the two isomorphs the prediction obtained using the isomorph invariance of $\tilde{\eta}$ in conjunction with data for the viscosity at the lowest-density state point (black triangles), as well as the prediction of the viscosity equation (10) of Ref. 58.

In summary, a constant hydrodynamic diameter is inconsistent with hidden scale invariance and cannot apply for the LJ system or any other R-simple system. In order to explain the observed SE breakdown, there is no need to invoke a varying hydrodynamic diameter. We have given an approximate analytical description of the SE breakdown, making it possible from the diffusion coefficient to predict the viscosity of the LJ system at state points above the critical density. It is not clear whether it is possible to extend these findings to lower densities where the isomorph theory is not expected to work.

This work was supported by the VILLUM Foundation’s Matter grant (No. 16515).

REFERENCES

- ¹M. P. Allen and D. J. Tildesley, *Computer Simulation of Liquids* (Oxford University Press, 1986).
- ²W. T. Ashurst and W. G. Hoover, *Phys. Rev. A* **11**, 658 (1975).
- ³N. H. March and M. P. Tosi, *Introduction to Liquid State Physics* (World Scientific, 2002).
- ⁴W. Sutherland, *London Edinburgh Dublin Philos. Mag.* **9**, 781 (1905).
- ⁵J. T. Hynes, *Annu. Rev. Phys. Chem.* **28**, 301 (1977).
- ⁶M. Cappelezzo, C. A. Capellari, S. H. Pezzin, and L. A. F. Coelho, *J. Chem. Phys.* **126**, 224516 (2007).
- ⁷J. C. M. Li and P. Chang, *J. Chem. Phys.* **23**, 518 (1955).
- ⁸J. T. Edward, *J. Chem. Educ.* **47**, 261 (1970).
- ⁹T. G. Hiss and E. L. Cussler, *AIChE J.* **19**, 698 (1973).
- ¹⁰D. F. Evans, T. Tominaga, and C. Chan, *J. Solution Chem.* **8**, 461 (1979).
- ¹¹H. T. Davis, T. Tominaga, and D. F. Evans, *AIChE J.* **26**, 313 (1980).
- ¹²H. J. V. Tyrell and K. R. Harris, *Diffusion in Liquids* (Butterworths, London, 1984).
- ¹³D. Chandler, *J. Chem. Phys.* **62**, 1358 (1975).
- ¹⁴D. Lavalette, C. Tétreau, M. Tourbez, and Y. Blouquit, *Biophys. J.* **76**, 2744 (1999).
- ¹⁵Y. P. Sun and J. Saitiel, *J. Phys. Chem.* **93**, 8310 (1989).
- ¹⁶W. J. Lamb, G. A. Hoffman, and J. Jonas, *J. Chem. Phys.* **74**, 6875 (1981).
- ¹⁷F. Ould-Kaddour and D. Levesque, *Phys. Rev. E* **63**, 011205 (2001).
- ¹⁸D. M. Heyes, *J. Phys.: Condens. Matter* **19**, 376106 (2007).
- ¹⁹D. M. Heyes, M. J. Nuevo, and J. J. Morales, *Mol. Phys.* **93**, 985 (1998).
- ²⁰J. R. Schmidt and J. L. Skinner, *J. Phys. Chem. B* **108**, 6767 (2004).
- ²¹M. G. McPhie, P. J. Daivis, and I. K. Snook, *Phys. Rev. E* **74**, 031201 (2006).
- ²²D. M. Heyes, M. J. Nuevo, J. J. Morales, and A. C. Branka, *J. Phys.: Condens. Matter* **10**, 10159 (1998).
- ²³D. M. Heyes, M. J. Nuevo, and J. J. Morales, *J. Chem. Soc., Faraday Trans.* **94**, 1625 (1998).
- ²⁴D. M. Heyes, M. J. Cass, J. G. Powles, and W. A. B. Evans, *J. Phys. Chem. B* **111**, 1455 (2007).
- ²⁵G. Tarjus and D. Kivelson, *J. Chem. Phys.* **103**, 3071 (1995).
- ²⁶S. K. Kumar, G. Szamel, and J. F. Douglas, *J. Chem. Phys.* **124**, 214501 (2006).
- ²⁷F. Puosi, A. Pasturel, N. Jakse, and D. Leporini, *J. Chem. Phys.* **148**, 131102 (2018).
- ²⁸U. Balucani, R. Vallauri, T. Gaskell, and M. Gori, *J. Phys. C: Solid State Phys.* **18**, 3133 (1985).
- ²⁹U. Balucani, G. Nowotny, and G. Kahl, *J. Phys.: Condens. Matter* **9**, 3371 (1997).
- ³⁰K. Rah and B. C. Eu, *Phys. Rev. E* **60**, 4105 (1999).
- ³¹R. Zwanzig and A. K. Harrison, *J. Chem. Phys.* **83**, 5861 (1985).
- ³²C. Wakai and H. Nakahara, *J. Chem. Phys.* **100**, 8347 (1994).
- ³³K. R. Harris, *J. Chem. Phys.* **131**, 054503 (2009).
- ³⁴G. L. Pollack and J. J. Enyeart, *Phys. Rev. A* **31**, 980 (1985).
- ³⁵J. C. Dyre, T. Christensen, and N. B. Olsen, *J. Non-Cryst. Solids* **352**, 4635 (2006).
- ³⁶F. Demmel and A. Tani, *Phys. Rev. E* **97**, 062124 (2018).
- ³⁷N. H. March and M. P. Tosi, *Phys. Rev. E* **60**, 2402 (1999).
- ³⁸N. H. March and J. A. Alonso, *Phys. Rev. E* **73**, 032201 (2006).
- ³⁹R. Zwanzig, *J. Chem. Phys.* **79**, 4507 (1983).
- ⁴⁰T. Gaskell, *Phys. Lett. A* **90**, 51 (1982).
- ⁴¹F. Dullien, *AIChE J.* **18**, 62 (1972).
- ⁴²U. Mohanty, *Phys. Rev. A* **32**, 3055 (1985).
- ⁴³H. Eyring and T. Ree, *Proc. Natl. Acad. Sci. U. S. A.* **47**, 526 (1961).
- ⁴⁴N. Ohtori and Y. Ishii, *Phys. Rev. E* **91**, 012111 (2015).
- ⁴⁵N. Ohtori, H. Uchiyama, and Y. Ishii, *J. Chem. Phys.* **149**, 214501 (2018).
- ⁴⁶N. Jakse and A. Pasturel, *J. Chem. Phys.* **144**, 244502 (2016).
- ⁴⁷Y. Rosenfeld, *Phys. Rev. A* **15**, 2545 (1977).
- ⁴⁸J. E. Lennard-Jones, *Proc. R. Soc. London, Ser. A* **106**, 441 (1924).
- ⁴⁹J. C. Dyre, *J. Phys.: Condens. Matter* **28**, 323001 (2016).
- ⁵⁰D. M. Heyes, *Comput. Methods Sci. Technol.* **21**, 169 (2015).
- ⁵¹R. Agrawal and D. A. Kofke, *Mol. Phys.* **85**, 43 (1995).
- ⁵²N. P. Bailey, T. S. Ingebrigtsen, J. S. Hansen, A. A. Veldhorst, L. Bøhling, C. A. Lemarchand, A. E. Olsen, A. K. Bacher, L. Costigliola, U. R. Pedersen, H. Larsen, J. C. Dyre, and T. B. Schröder, *SciPost Phys.* **3**, 038 (2017).
- ⁵³L. Costigliola, T. B. Schröder, and J. C. Dyre, *Phys. Chem. Chem. Phys.* **18**, 14678 (2016).
- ⁵⁴D. J. Evans and G. Morriss, *Statistical Mechanics of Nonequilibrium Liquids* (Cambridge University Press, 2008).
- ⁵⁵P. J. Daivis and B. D. Todd, *J. Chem. Phys.* **124**, 194103 (2006).
- ⁵⁶M. W. Evans and D. M. Heyes, *Mol. Phys.* **69**, 241 (1990).
- ⁵⁷L. Costigliola, U. R. Pedersen, D. M. Heyes, T. B. Schröder, and J. C. Dyre, *J. Chem. Phys.* **148**, 081101 (2018).
- ⁵⁸N. Gnan, T. B. Schröder, U. R. Pedersen, N. P. Bailey, and J. C. Dyre, *J. Chem. Phys.* **131**, 234504 (2009).
- ⁵⁹J. C. Dyre, *J. Phys. Chem. B* **118**, 10007 (2014).
- ⁶⁰T. S. Ingebrigtsen, T. B. Schröder, and J. C. Dyre, *Phys. Rev. X* **2**, 011011 (2012).
- ⁶¹P. G. Debenedetti, *J. Phys.: Condens. Matter* **15**, R1669 (2003).
- ⁶²U. R. Pedersen, L. Costigliola, N. P. Bailey, T. B. Schröder, and J. C. Dyre, *Nat. Commun.* **7**, 12386 (2016).
- ⁶³L. Bøhling, T. S. Ingebrigtsen, A. Grzybowski, M. Paluch, J. C. Dyre, and T. B. Schröder, *New J. Phys.* **14**, 113035 (2012).
- ⁶⁴T. S. Ingebrigtsen, L. Bøhling, T. B. Schröder, and J. C. Dyre, *J. Chem. Phys.* **136**, 061102 (2012).